

## TECHNICAL REPORT

# A Novel Instrument for Studying the Flow Behaviour of Erythrocytes through Microchannels Simulating Human Blood Capillaries

N. Sutton,\* M. C. Tracey,† I. D. Johnston,†  
R. S. Greenaway,† and M. W. Rampling\*

\*Department of Physiology and Biophysics, Imperial College School of Medicine at St Mary's, London W2 1PG, United Kingdom; and †Engineering Research and Development Centre, University of Hertfordshire, Hatfield, Hertfordshire AL10 9AB, United Kingdom

Received July 31, 1996

A novel instrument has been developed to study the microrheology of erythrocytes as they flow through channels of dimensions similar to human blood capillaries. The channels are produced in silicon substrates using microengineering technology. Accurately defined, physiological driving pressures and temperatures are employed whilst precise, real-time image processing allows individual cells to be monitored continuously during their transit. The instrument characterises each cell in a sample of ca. 1000 in terms of its volume and flow velocity profile during its transit through a channel. The unique representation of the data in volume/velocity space provides new insights into the microrheological behaviour of blood. The image processing and subsequent data analysis enable the system to reject anomalous events such as multiple cell transits, thereby ensuring integrity of the resulting data. By employing an array of microfluidic flow channels we can integrate a number of different but precise and highly reproducible channel sizes and geometries within one array, thereby allowing multiple, concurrent, isobaric measurements on one sample. As an illustration of the performance of the system, volume/velocity data sets recorded in a microfluidic

device incorporating multiple channels of 100  $\mu\text{m}$  length and individual widths ranging between 3.0 and 4.0  $\mu\text{m}$  are presented. © 1997 Academic Press

## INTRODUCTION

### *Current Microrheological Techniques*

Two techniques have dominated haemorheological research in the single-cell regime: micropipette aspiration and filtration. There is extensive literature on the use of such techniques; however, a brief summary of their respective merits and drawbacks is presented here.

Micropipette aspiration (Paulitschke and Nash, 1993) is a very effective tool for examining both static and dynamic behaviour of erythrocytes on a single-cell basis and is particularly useful in the quantification of cyto-mechanical coefficients. Excellent results have been obtained for very small numbers of cells; however, because cells are studied individually and micropipette

fabrication reproducibility is relatively poor, their overall effectiveness in extensive microrheological studies is limited.

The basic filtration technique (Reinhart *et al.*, 1984; Nash, 1990) offers the potential to analyse large blood cell samples in very short time periods by use of a multipore polycarbonate membrane. The resultant data reflect only the average flow properties of the entire cell sample, as the technique is not able to resolve information relating to cell flow through a particular pore or resolve individual cell transits. Whilst efforts have been made to interpret further the results by fitting models to the bulk flow data (Evans *et al.*, 1993), it is clear that direct measurement of the cells is of greater ultimate resolution and accuracy.

Further development of the filtration technique has yielded a number of other refinements able to discriminate between single-cell transits. The Single Erythrocyte Rigidometer is based upon a single pore membrane and has used optical absorption (Kiesewetter *et al.*, 1982) and electrical conductivity techniques (Roggenkamp *et al.*, 1984) for cell transit detection. This latter use of the technique has evolved further with the application of a multipore membrane containing, typically, 30 pores: the Cell Transit Time Analyzer or CTTA (Koutsouris *et al.*, 1988). The use of multiple pores reduces the probability of total occlusion; however, the instrument cannot identify the pore through which a given cell passes and hence restricts any possibility of correcting data for anomalous behaviour in individual pores. By incorporating new software into the analysis sequence, Fisher *et al.* (1992) have attempted to examine the shape of the resistive pulse representing each erythrocyte transit through a CTTA pore. This technique has enabled further investigation into cell entrance and exit phenomena, allowing the complete pore transit time and hence cell mechanical behaviour to be considered more thoroughly.

A common factor among all these filtrometry-based instruments is the lack of any measure of individual cell volume, thereby rendering it difficult to distinguish changes in erythrocyte filtration due to the volume distribution within the erythrocyte sample from those due to intrinsically less deformable cells. A further disadvantage is that the vast majority of experiments are performed at suprphysiological pressure differentials

and in general do not satisfactorily mimic physiological conditions.

Foremost amongst other techniques employed to assess cell deformability, but not cell volume, is ektacytometry (Bessis and Mohandas, 1975). Such an instrument is commercially available from R & R Mechatronics, the Netherlands. This is a laser diffraction pattern technique which examines cells as they are subjected to varying shear rates. In its current state of development, the technique does not operate on a cell-by-cell basis as the laser beam illuminates a large number of cells simultaneously and again only an averaged cell deformability index is measured.

### *Techniques Employing Micromachining*

The applicability of micromachining to blood analysis in microchannels has previously been reported by a number of researchers (Kikuchi *et al.*, 1989, 1992; Tracey *et al.*, 1991, 1995; Cokelet *et al.*, 1993; Wilding *et al.*, 1994; Brody *et al.*, 1995). The work reported by Kikuchi *et al.* represents a very precise and reproducible filtrometer, commercially available from Hitachi Ltd., Haramachishi, Fukushima-ken, Japan. It is based on a silicon device containing 2600 triangular cross section grooves of typically 6  $\mu\text{m}$  equivalent diameter (compared with circular channels) and 14.4  $\mu\text{m}$  length. Measurements performed are similar to those using Nucleopore filtration techniques; however, two major differences between the methods are the precision of the silicon filter structure and the optical accessibility of the blood cells in the silicon grooves, allowing for visual observation, though not image analysis, of the entire passage of the cells through the grooves.

The device described by Cokelet *et al.* employs a network of circa 20  $\mu\text{m}$  diameter, circular or elliptical channels (depending on actual channel diameter) etched into glass, thus rendering the channels transparent and allowing for the blood flow to be video recorded. Whilst no system of fluidic control is presented, there exists the potential of incorporating the glass devices into a more complete unit for investigating flow patterns through *in vitro* vascular circuits and thus enabling validation of theoretical flow analyses.

Wilding *et al.* also report the use of silicon channels with dimensions emulating larger microvasculature.

They employed a structure consisting of 11.7-mm-long, straight channels with widths between 40 and 100  $\mu\text{m}$  and depths between 20 and 40  $\mu\text{m}$ . Due to the relatively large channel dimensions, the bulk flow properties of various blood cell suspensions rather than single-cell mechanics were investigated.

Brody *et al.* report the use of a microfluidic device consisting of repeated arrays of 12  $\mu\text{m}$  long  $\times$  4  $\mu\text{m}$  wide  $\times$  4  $\mu\text{m}$  deep channels. They investigate their interesting hypothesis that erythrocyte mechanical moduli change dynamically in response to cell deformation. Their elementary experimental configuration was not reported to provide a precision fluid control system or real-time image processing (static image processing was employed). Significantly, contrary to results reported here, Brody *et al.* report an absence of any effective correlation between cell diameter and flow velocity.

### ***Silicon Micromachined Haemocytometer***

From the preceding discussion, we conclude that there is still a need for a haemocytometer which can measure a large cell sample size in the single-cell flow regime under physiological conditions of pressure and temperature. The instrument should provide a full record of every cell's passage through a precisely defined region including a measure of the cell's volume and a full transit profile under both static and dynamic deformation conditions. These principles have been implemented in the instrument presented in this report.

The instrument exploits the manufacturing process of silicon micromachining to produce flow devices consisting of an array of precisely defined microflow channels. Cell monitoring is performed by a sophisticated image analysis system. The integration of these components into a complete haemorheological measurement system is described below. Whilst a comprehensive account of the instrument, including device fabrication techniques, is detailed elsewhere (Tracey *et al.*, 1995), a brief overview of the system will be presented by way of a review and an update. The system essentially consists of three fundamental elements: a fluidic system (incorporating microfluidics), an image acquisition and image processing subsystem, and data processing software.

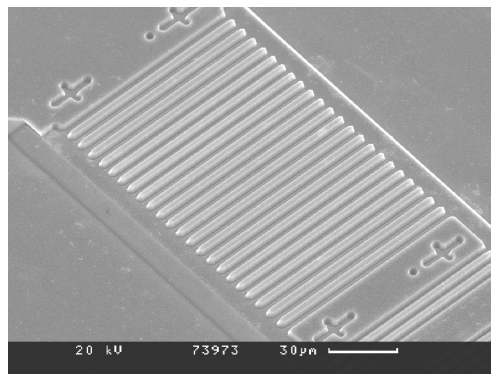


FIG. 1. Detail of a multiwidth channel array showing groups of six channels, each taking a width between 3.0 and 4.0  $\mu\text{m}$ , in 0.2- $\mu\text{m}$  increments.

## **MATERIALS AND METHODS**

### ***Micromachined Haemocytometer Operation: Fluidics***

The instrument is centred around a bulk silicon micromachined flow device consisting of an array of flow channels with typical dimensions of 4  $\mu\text{m}$  width and depth and 100  $\mu\text{m}$  length. The channels are similar in both length and cross sectional area (but not, as yet, profile) to their physiological equivalents. Currently implemented topologies range from straight, constant width channels (Fig. 1) to channels with precise constrictions and channels with continually varying width. These different channel topologies have been incorporated into a single device enabling concurrent measurements of erythrocytes in a range of different environments.

The channels open out into deeper fluidic coupling reservoirs of 15  $\mu\text{m}$  depth which convey cells between the channels and two pairs of feedshafts, one in the input and one in the output reservoir of the device. A typical device is shown in Fig. 2.

Fluidic sealing is achieved by attaching a glass cover to the top of the device by the process of anodic bonding. The composite device is mounted onto a small printed circuit board (PCB) along with a series of heating resistors, a solid-state temperature sensor, and other surface-mount components to which the device is ther-

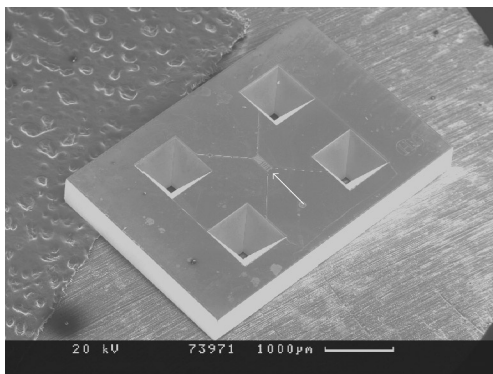


FIG. 2. General view of a device showing the channel array in the centre of the picture and the four feed shafts which couple the device to a macrofluidic circuit. Overall device dimensions are  $3.3 \times 4.9 \times 0.5$  mm.

mally coupled, providing a closed-loop  $37^\circ$  heating system. This ensures that measurements are performed at physiological temperatures.

Fluid is introduced into the device feedshafts via  $250\text{-}\mu\text{m}$  bore nylon tubing attached to the underside of the PCB. This tubing connects the device to a macrofluidic system which addresses a number of fluidic issues. These include the establishment of a bubble-free fluidic circuit, provision of high device priming pressures, and the maintenance of a low hydrostatic pressure which determines cell flow through the channels. These functions are implemented by 22 computer-controlled fluid and pneumatic valves which facilitate precise fluid control (Fig. 3).

Priming of the fluidic circuit with a degassed fluid, performed under  $50$  kPa pneumatic pressure, is necessary for the formation of a complete fluidic pathway within all fluid components of the system, and enables the establishment of a bubble-free fluid environment. During this priming phase, the operating hydrostatic pressure is initially zeroed in preparation for erythrocyte measurement.

The erythrocyte suspension is introduced into the fluid system from the analyte chamber R3 (Fig. 3) and pumped closer to the device through the feed tubing, under  $2$  kPa of pressure. The cells are then pumped through the device input reservoir under a lower pneumatic pressure, preparing them for measurement within the channels. This flow is stopped when there

is a suitable number of cells within the device input reservoir. A channel pressure differential is then applied, forcing the cells through the channels. Cell flow through the channels is regulated by offsetting the previously established hydrostatic pressure equilibrium by means of a computer-controlled, servo-driven lead screw lifting the hydrostatic head vessel. The hydrostatic head height can be adjusted in  $25\text{-}\mu\text{m}$  steps, resulting in channel pressure differentials of between  $-3$  and  $+25$  mmH<sub>2</sub>O with respect to the equilibrium value. The particular measurement sequence is ended when the cell supply in the reservoir is exhausted. The input reservoir then undergoes another low-pressure blood prime and is filled with the next batch of cells ready for further measurement, under different conditions if required.

By virtue of the multiple, concurrent measurements that may be performed within the channel array, it is possible to integrate a number of different, precise channel dimensions and profiles within one array, thereby enabling true, isobaric, isothermal measurements on a significant erythrocyte sample size.

### ***Micromachined Haemocytometer Operation: Image Acquisition and Processing***

Figure 4 shows, inter alia, details of the cell imaging system. The system employs incident illumination microscopy with monochromatic light, thereby exploiting contrast enhancement due to selective absorption by intracellular haemoglobin at a  $400\text{-nm}$  wavelength. This causes the cells to appear as dark objects against the highly reflective background of the silicon channels (Fig. 5). A  $40\times$ ,  $0.65$  NA refracting objective is used to image the channels onto a monochrome CCD video camera. The resulting video sequences can be processed in real-time or stored for later processing. Image processing and the real-time analysis are performed by custom written software.

Image processing is notoriously computationally intensive, and this is exacerbated by our requirement of fully interpreting each video frame in real-time. We have addressed this issue by developing highly efficient processing algorithms and by implementing these algorithms on a separate high-speed ‘‘DSP’’ processor mounted within the host PC.

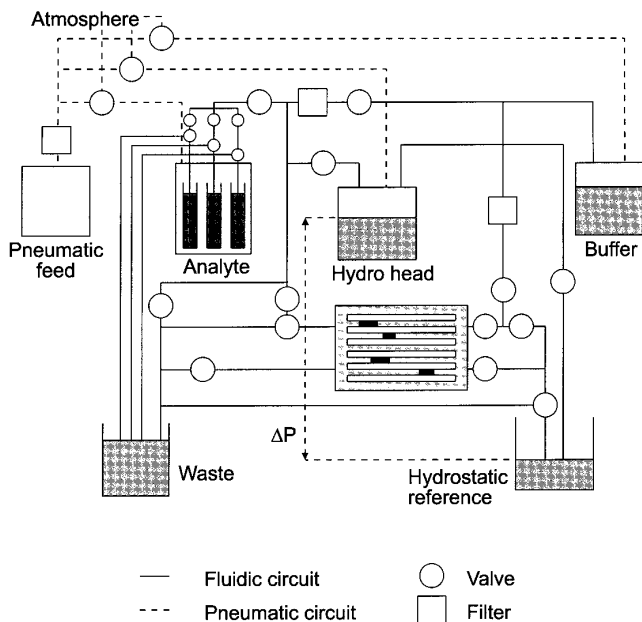


FIG. 3. The macrofluidic system used to control flow through the silicon device.  $\Delta P$  represents the pressure differential across the channels.

The objective of the image processing is to scan each channel, in each video frame, for the presence of cells and track them through subsequent frames until they exit. Currently, between 10 and 14 channels can be imaged at any one time, depending on the width of the channels in the particular device being employed. The two parameters sought during tracking are the cell's centroid in the imaging plane, from which a velocity profile and thus a mean velocity can be determined, and a measurement of the optical density of the erythrocyte from which its volume can be calculated.

Volume measurement is a specific area of the image processing which has been refined greatly since previous reports of the instrument (Tracey *et al.*, 1995). It is now measured via the use of a highly complex algorithm which first locates each erythrocyte in each video frame and then, using true "grey-scale" imaging methods, calculates the integrated optical density of the haemoglobin-containing stroma of the erythrocyte. An intrinsic calibration technique based on knowledge of the volume of a three-dimensional video pixel of known optical density enables the erythrocyte optical density

information to be converted into a measure of true erythrocyte volume.

During this real-time stage of the processing, every object which is imaged in the channels is monitored and its data is stored. Further interpretation of this raw data is performed during a separate data processing sequence subsequent to the real-time analysis.

### **Micromachined Haemocytometer Operation: Data Processing**

Data processing acts on the raw data output by the preceding image processing sequence and involves extracting the data from its compressed form to perform the required velocity and volume calculations whilst rejecting spurious data arising from various events within the channels during operation. Ideally, there would be a mean channel occupancy of one cell in each channel of the monitored array at any one time. Whilst adjustment of the cell sample haematocrit provides an approximation to this situation, it is not achieved throughout the duration of a particular experiment due to complex microflow patterns within the device. Too high an haematocrit results in multiple cell transits through channels (Fig. 5) and hence the pressure differential across the individual cells within the affected channels is not defined. This would result in spurious data, particularly in terms of cell velocity; however, these occurrences are filtered out during the data processing sequence as measurements are only made on those channels containing single cells.

Data integrity is further ensured by enforcing upper and lower limits to the valid cell volume in the data processing software. This filters out transits of objects which do not fit within the specified range and is particularly useful in identifying occurrences when two or more cells move through the channel in very close proximity such that they appear as a single object. The software identifies this as an anomalous object and thus data associated with these cells are not presented in the final statistics. Careful choice of minimum and maximum volumes results in minimal, if any, false rejection of valid data and in a very high degree of confidence that maximum information representing true erythrocyte transits is obtained from the experiment. The numerical information output for each valid cell consists

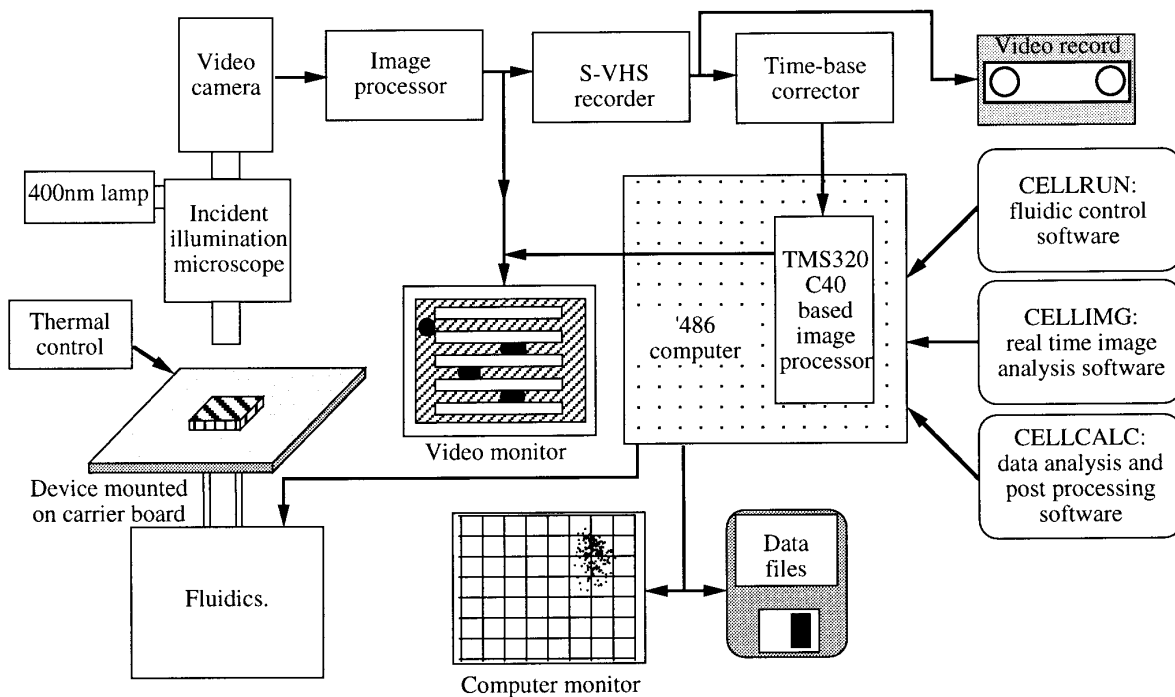


FIG. 4. Overview of the instrument showing the fluid control, image analysis, and image processing elements.

of the volume, velocity profile, channel identification number, and the time at which the cell entered the channel.

### Blood Preparation

Fifteen milliliters of blood was taken by venepuncture from a healthy adult. Five milliliters was anticoagulated with heparin (12.5 IU/ml) and the rest placed in a glass centrifuge tube and allowed to clot for 30

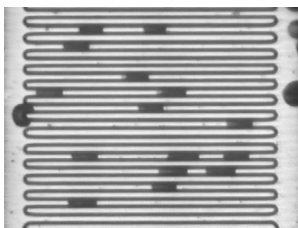


FIG. 5. Image of erythrocytes flowing through a channel array, showing examples of single-, double-, and triple-cell transits.

min. The latter sample was then centrifuged and the supernatant autologous serum removed and stored. The heparinised sample was also centrifuged and the plasma along with the surface buffy coat of leucocytes and platelets was removed and discarded. The remaining erythrocytes were then subjected to three washes with 0.2- $\mu$ m filtered isotonic phosphate-buffered saline (PBS: 3.45 g/liter  $\text{Na}_2\text{HPO}_4$ ; 0.776 g/liter  $\text{KH}_2\text{PO}_4$ ; 7.072 g/liter NaCl; 0.1 g/liter  $\text{NaN}_3$ ; osmolarity, 290 mOsmol/liter; pH 7.40) by repeated centrifugation and resuspension. This removed all plasma proteins from the suspension. After the final centrifugation, cells were aspirated from the entire length of the packed erythrocyte column and then suspended at a haematocrit of approximately 5% in PBS containing 25% (v/v) of the previously collected autologous serum. This mixed buffer was also filtered to 0.2  $\mu$ m prior to use. All erythrocyte measurements were made within 6 hr of blood sampling and the erythrocyte suspensions were stored at room temperature until measurement commenced. All centrifugations of the samples were performed at 3000 rpm for 5 min.

## System Preparation

Initial priming of the fluidic circuit was performed using PBS containing 1% w/v bovine serum albumin (Sigma, St. Louis, MO). This step also serves to precoat the silicon surface of the device with protein which, with the addition of autologous serum to the erythrocyte suspension, inhibits cell-silicon surface adhesion and maintains cell morphology (Persson and Larsson, 1991). The final PBS/BSA solution was filtered to  $5\ \mu\text{m}$  before use.

Upon completion of circuit priming and the establishment of a bubble-free fluid path, erythrocyte measurements were conducted in a device containing an array of  $100\text{-}\mu\text{m}$ -long and  $3.2\text{-}\mu\text{m}$ -deep channels, each of a constant width. The device consisted of a repeated group of six different channels, each having a constant width between  $3.0$  and  $4.0\ \mu\text{m}$  with channel width increments of  $0.2\ \mu\text{m}$ . A range of pressure differentials between  $5$  and  $15\ \text{mmH}_2\text{O}$  was employed to produce cell flow through the channels and each group of sample measurements was obtained over a time period of between  $3$  and  $5$  min.

## RESULTS

As discussed previously the data output consists of, inter alia, volume and velocity information for every erythrocyte in the measured sample. The plots in Fig. 6 are typical examples of some of the unique information that is yielded from an experiment. They illustrate data obtained using one of five operating pressures for 3 of the 14 flow channels chosen for imaging during the experiment and hence represent just a small part of the experiment's total data output. One salient point to be made here is that the data for the three plots were collected concurrently, under isobaric conditions. This particular sample run was conducted at a constant channel pressure differential of  $9\ \text{mmH}_2\text{O}$ .

The most distinct observation to be made from the plots is the existence of clear, highly significant ( $P < 0.0005$ ), negative, linear correlations between volume and mean erythrocyte velocity for all of the channel widths. The other notable point is the clear ability to discern the increase in the mean velocity of the entire erythrocyte sample with increasing channel width. Such fine discrimination is possible only by virtue of the

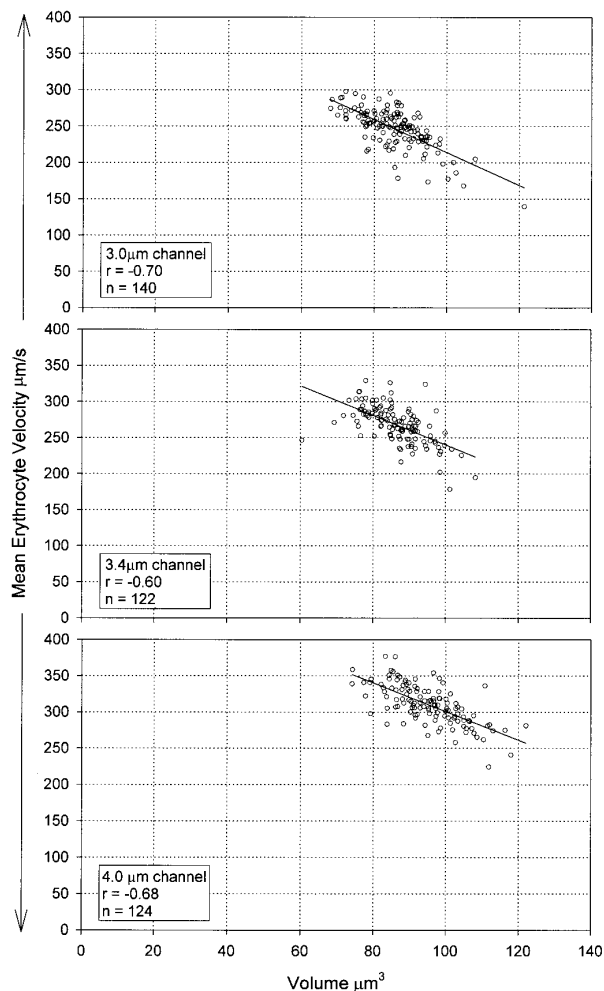


FIG. 6. Sequence of erythrocyte mean velocity/volume index scatterplots for  $3.0$ -,  $3.4$ -, and  $4.0\text{-}\mu\text{m}$  width channels. Each datum point represents a single erythrocyte. The data were recorded concurrently in a multichannel width analysis device at a pressure differential of  $9\ \text{mm H}_2\text{O}$ . All correlations are highly significant ( $P < 0.0005$ ).

precision microengineering and the concurrent, hence isobaric, nature of the measurement. It should be noted that in terms of volume measurement, the instrument was calibrated against the mean cell volume of the erythrocyte sample as measured by a Technicon H2 flow cytometer.

## DISCUSSION

The results we have presented report for the first time the quantitative inverse relationship between the

volume and the velocity of erythrocytes as they pass through narrow channels. The unique manner of measurement and two-dimensional data representation based on a cell-by-cell approach enables us to evaluate independently some of the mechanisms involved in erythrocyte deformation. This unique method is in sharp contrast to existing microrheological techniques such as the CTTA, which can often be ambiguous in their discrimination between intrinsic and extrinsic cell deformability characteristics. Such instruments measure the filterability rather than the deformability of erythrocytes.

The filterability of an erythrocyte is a function of both its intrinsic deformability *and* its volume, i.e., it is volume dependent, and therefore to examine the contribution of cellular deformability requires that the cell's volume should first be quantified. This cannot be achieved with the one-dimensional data representation of filterometers such as the CTTA, which expresses filtration in terms of pore transit time histograms (Koutsouris *et al.*, 1988).

An explicit example of the poor resolution of filterometers is their inability to distinguish larger normal cells, which may have longer transit times simply because of their size, from abnormal smaller cells, which may have longer transit times because they are intrinsically less deformable. Accordingly, data from filterometers is often combined with erythrocyte sample *mean* cell volume information (Reinhart *et al.*, 1984; Reinhart, 1992); however, at best this still only enables the *average* behaviour of two or more samples to be compared, hence offering little infrastructural insight into the deformability of erythrocytes within a single sample. Figure 6 illustrates clearly the unique two-dimensional volume/velocity data representation which overcomes these deficiencies and distinguishes this new instrument from existing filtration techniques.

Whilst *qualitatively* the inverse relationship between erythrocyte volume and velocity we report is not surprising, we feel that it is imperative that the behaviour of normal erythrocytes is characterised fully in a *quantitative* manner before we can employ the instrument in cytomechanical and pathophysiological studies. An obvious example of such a project is the investigation of the mechanical behaviour of pathological erythrocytes where the possible existence of subpopulations of more

rigid cells and/or abnormally sized cells can be discerned only by first recognising the volume/velocity characteristics of a normal erythrocyte sample.

Detection of abnormal or pathological cell behaviour requires that the instrument has a high degree of resolution and sensitivity. An example of these attributes is illustrated in Fig. 6. Considering the top plot of the figure, there is a clear, possibly suspect, outlier. As part of the data output includes a channel number and entry time for each measured object, it is possible to examine closely the video recording of an experiment and identify each "cell" transit. Examination of the video tape corresponding to the outlier revealed that it was, in fact, a perfectly valid, though obviously large erythrocyte and hence this data was not rejected from the plot.

This illustrates the very powerful nature of the image analysis and image processing sequence. We can be very confident that each point on the plots represents a valid measurement of a true erythrocyte and thus the results are not permeated with ambiguous data.

### Further Work

Though it is apparent that the technique has the potential to offer high intra- and interexperimental reproducibility, we are conscious that the complexity of the technique mandates a rigorous evaluation of these properties prior to conducting formal haemorheological measurements, in particular where these involve multiple, comparative experiments. Accordingly, we are commencing a detailed statistical analysis of our experimental data. This is in terms of interchannel reproducibility for nominally identical channels within one device and also in terms of interdevice reproducibility. Our preliminary analyses indicate that good volume and velocity reproducibility can be obtained in both contexts; however, our volume reproducibility requires improvement in other circumstances. The main area of volume measurement discrepancy to be investigated concerns erythrocyte flow through channels of different widths. Each channel within an array effectively represents a single experiment as the erythrocyte data are obtained for each channel independently. The measurement of erythrocyte volume is consistent within a single channel and within a group of channels of the same size. This is not yet the case, however,



for groups of channels of different widths and hence volume comparisons of erythrocytes between such channels may not be valid. Accordingly, we currently treat the data from each channel independently and thus the plots in Fig. 6 represent true volume/velocity relationships for each particular channel.

Whilst the work reported here concerns flow determined (in cellular terms) by static cell-mechanical moduli, the techniques of channel microfabrication lend themselves to the creation of more sophisticated channels such as those with stepped widths, constrictions, and sinusoidally varying wall profiles, which have been the subject of recent theoretical modelling (Secomb and Hsu, 1996). Such structures provide the means to investigate the dynamic behaviour of cell deformation in a highly defined manner. We are currently fabricating devices with channel arrays consisting of multiple topologies, including those mentioned above.

## Conclusions

We consider that traditional instruments used to measure microhaemorheological properties are not of sufficient resolution to investigate single erythrocyte flow. They are limited, each to a different degree, by several issues including a lack of fabrication accuracy and reproducibility, a lack of precision fluid control, failure to examine individual cells, and failure to provide a measure of cell volume: a necessity in the cell-by-cell investigation of the deformability of a significant erythrocyte sample.

The emerging technology of silicon micromachining, which offers very high levels of fabrication accuracy and versatility appropriate to the haemorheological field, has been employed by a number of researchers. Hitherto, however, the technology has not been integrated into a complete instrument capable of fully circumventing the disadvantages of other techniques.

We have presented an integral system of precise fluidic control, micromachined flow channels, and real-time image processing to measure erythrocyte flow through environments of microvascular dimensions, at physiological pressures and temperature. Paired volume and velocity data can be presented for each measured erythrocyte through a range of channel sizes and profiles in a sample of ca. 1000 cells, allowing a unique

interpretation of erythrocyte flow. Initial results illustrate highly significant negative correlations between cell volume and velocity, a result not previously reported in the literature due to the severely limited volume measure, if any, offered by other techniques.

Our preliminary results indicate strongly that the instrument described herein represents a powerful new tool to investigate the cell-by-cell flow and deformation properties of erythrocytes in the microvascular regime in an unambiguous manner and to a degree previously unobtainable.

## ACKNOWLEDGMENTS

We acknowledge the assistance of: Dr. A. J. Barnes M.D. for his unstinting advice and support; Christian Schön, Carsten Kleinstueber, and Prof. W. Dötzel of Technische Universität, Chemnitz-Zwickau, Germany; Prof. R. Lawes of the Central Microstructure Facility, Rutherford Appleton Laboratory, Oxfordshire, UK; Dr. Vishal Nayar, Defence Research Agency, Malvern, UK; and Dr. John Greenwood, Druck Ltd, Groby, Leicestershire, UK, all for their assistance in silicon microfabrication. We also thank Bill Liley, University of Hertfordshire, for the provision of SEM facilities. Finally, we acknowledge the financial support of The British Heart Foundation, Grant PG/94123, The Wellcome Trust, Grant 040430A94A, and the British Council.

## REFERENCES

- Bessis, M., and Mohandas, N. (1975). A diffractometric method for the measurement of cellular deformability. *Blood Cells* **1**, 307–313.
- Brody, J. P., Han, Y., Austin, R. H., and Bitensky, M. (1995). Deformation of flow and red blood cells in a synthetic lattice: Evidence for an active cytoskeleton. *Biophys. J.* **88**, 2224–2232.
- Cokelet, G. R., Soave, R., Pugh, G., and Rathbun, L. (1993). Fabrication of in vitro microvascular blood flow systems by photolithography. *Microvasc. Res.* **46**, 394–400.
- Evans, S. A., Jones, J. G., Wardrop, C. A. J., and Lane, I. (1993). Leucocyte filterability in peripheral vascular diseases. *Clin. Hemorheol.* **10**, 73–81.
- Fisher, T. C., Wenby, R. B., and Meiselman, H. J. (1992). Pulse shape analysis of RBC micropore flow via new software for the cell transit analyser (CTA). *Biorheology* **29**, 185–201.
- Kiesewetter, H., Dauer, U., Teitel, P., Schmid-Schonbein, H., and Trapp, R. (1982). The single erythrocyte rigidometer (SER) as a reference for RBC deformability. *Biorheology* **19**(6), 737–753.
- Kikuchi, Y., Ohki, H., Kaneko, T., and Sato, K. (1989). Microchannels

- made on silicon wafer for measurement of flow properties of blood cells. *Biorheology* **26**, 1055.
- Kikuchi, Y., Sato, K., Ohki, H., and Kaneko, T. (1992). Optically accessible microchannels formed in a single-crystal silicon substrate for studies of blood rheology. *Microvasc. Res.* **44**, 226–239.
- Koutsouris, D., Guillet, R., Lelievre, J. C., Boynard, M., Guillemin, M. T., Bertholom, P., Wenby, R. B., Beuzard, Y., and Meiselman, H. J. (1988). Individual red blood cell transit times during flow through cylindrical micropores. *Clin. Hemorheol.* **8**, 453–459.
- Nash, G. B. (1990). Filterability of blood cells: Methods and clinical applications. *Clin. Hemorheol.* **10**, 353–362.
- Paulitschke, M., and Nash, G. B. (1993). Micropipette methods for analysing blood cell rheology and their application to clinical research. *Clin. Hemorheol.* **13**, 407–434.
- Persson, S. U., and Larsson, H. (1991). Studies on red cell filterability: Significance of buffer media. *Clin. Hemorheol.* **11**, 317–324.
- Reinhart, W. H. (1992). The influence of iron deficiency on erythrocyte deformability. *Br. J. Haematol.* **80**, 550–555.
- Reinhart, W. H., Usami, S., Schmalzer, E. A., Lee, M. M. L., and Chien, S. (1984). Evaluation of red blood cell filterability test: Influences of pore size, hematocrit level, and flow rate. *J. Lab. Clin. Med.* **104**, 501–516.
- Roggenkamp, H. G., Jung, F., Schneider, R., and Kiesewetter, H. (1984). A new device for the routine measurement of erythrocyte deformability. *Biorheology Suppl.* **1**, 241–243.
- Secomb, T. W., and Hsu, R. (1996). Motion of red blood cells in capillaries with variable cross-sections. *J. Biomech. Eng.* **118**, 538–544.
- Tracey, M. C., Greenaway, R. S., Das, A., Kaye, P. H., and Barnes, A. J. (1995). A silicon micromachined device for use in blood cell deformability studies. *IEEE Trans. Biomed. Eng.* **42**(8), 751–761.
- Tracey, M. C., Kaye, P. H., and Shepherd, J. N. (1991). Microfabricated microhaemometer. In *Rec. 6th Int. Conf. Sensors and Actuators*, pp. 82–84. California.
- Wilding, P., Pfahler, J., Bau, H. H., Zemel, J. N., and Kricka, L. J. (1994). Manipulation and flow of biological fluids in straight channels micromachined in silicon. *Clin. Chem.* **40**(1), 43–47.